

# A Local Adaptive Segmentation of Vascular Network From Abnormal Retinal Images

Zhangwei Jiang  
University of Chinese  
Academy of Sciences  
Beijing, China  
jzwei023@gmail.com

Jing He  
Yanchun Zhang  
School of Engineering and Science  
Victoria University, Australia  
{Jing.He,Yanchun.Zhang}@vu.edu.au

Shang Hu  
University of Chinese  
Academy of Sciences  
Beijing, China  
hs277100042@qq.com

**Abstract**—Diabetes, hypertension, cerebral arteriosclerosis and other diseases have become great threats to human health, so it is urgent to explore their initial symptoms for early prevention and treatment. As an important part of small and medium-sized vessels of human body, retinal vessel is the only deep capillary that can be non-traumatic directly observed and its morphology, such as vascular diameter, shape and distribution, is deeply influenced by these diseases. So an effective vascular detection and features measurement will help make more accurate diagnosis of these diseases.

This paper proposes a local adaptive segmentation to detect more accurate retinal vascular network from abnormal retinal images which contain red and bright lesions. The retinal image is firstly segmented by weighted entropy with probability segmentation to detect preliminary vascular network. Then a two-dimensional partial differential matched filter is introduced into segmentation to differentiate lesions from vascular network based on a vascular property. The algorithm has been tested and compared with other vascular network segmentation algorithms on the publicly available STARE database since it contains retinal images where the vascular structure has been precisely marked by two experts. The experiments demonstrate that our approach is capable of detecting the vascular network effectively, offering a better segmentation results, especially on abnormal cases. Because of its effectiveness, simplicity and robustness for different image conditions, it is suitable for automated vascular analysis.

**Keywords**—Vascular Network, matched filter, weighted entropy, partial differential.

## I. INTRODUCTION

The automatic analysis of retinal vascular network is a very important issue in many clinical investigations and scientific research related to vascular features. It can aid for diagnosis and treatment of diabetic retinopathy and hypertension glaucoma, obesity, arteriosclerosis and retinal artery occlusion, etc. Information about vascular network in retinal images can be used in grading disease severity or as part of the process of automated diagnosis of these diseases. Changes in retinal morphology can reflect the occurrence and development process of diseases to some extent. We can use digital fundus photography and image analysis of retinal vascular morphology to find the relationship between changes in vascular morphology and development of diabetes. A segmentation of the vascular tree seems to be the most appropriate representation for the image registration applications due to three following reasons: 1) it maps the whole retina; 2) it does not move except in few

diseases; 3) it contains enough information for the localization of some anchor points [1].

Many vascular network detection methods have been reported in the literature. Most of these work can be roughly categorized into four main groups: window-based approach, classifier-based approach, tracking-based approach and active contour model. 1) *Window-based approach*: Chaudhuri [2] proposed matched filter to detect vascular network, which is based on the vascular gray-level characteristics. To better make use of the vascular features, Lin [3] used extended Kalman filter which takes into account continuities in curvature, width, and intensity changes at the bifurcation or crossover point to group vascular segments. Moreover, the method in [4] used oriented filters to calculate the filter response at various orientations by an efficient architecture to synthesize. These window-based methods decide whether a pixel belongs to vascular object mainly based on local characteristics of the pixel, regardless of global characteristics. 2) *Classifier-based approach*: Zana and Klein [5] presented a method based on mathematical morphology and linear processing for vascular recognition. To better preserve the spatial structures in the binarized/thresholded image, Chanwimaluang [1] proposed a local entropy thresholding scheme. However, the method easily classifies non-vascular pixels into vascular network despite in normal retinal images. To address the problem, Lau [6] modeled the segmented vascular structure as a vascular segment graph to find the optimal forest in the graph using an objective function. But it did not handle with non-vascular pixels in abnormal retinal images, such as the lesions. 3) *Tracking-based approach*: In [7], Wu and Stanchev proposed a method in which the ridges are detected by checking zero-crossing of the gradients and the curvature, and the tracking starts from the seed with the highest intensity. Also based on image ridges, Staal [8] introduced a system in which the image is partitioned into patches with line elements and tracking is done by assigning each image pixel to the closest line element. Different from the methods without manual intervention, Tramontan [9] proposed a system including an interactive editing interface to correct errors and set the required parameters of analysis after automatic vascular tracking. The tracking-based methods also only utilize the local related information for local search and depend on the choice of initial manually given starting point. 4) *Active contour model*: Shang [10] introduced a region competition-based active contour model exploiting the Gaussian mixture model to segment thick vessels

and Sun [11] proposed an active contour model using local morphology fitting with linear structuring element of adaptive scale and orientation for automatic vascular segmentation. The active contour model is among the most successful image segmentation technique in clinical applications, but it also needs the initial location manually and it is time-consuming for iteration.

Sumathy [12] proposed an entropy thresholding for vascular segmentation. But it did not make use of local information of the image and the lesions in abnormal images can not be differentiated from the vascular network by the method. In this paper, we use a weighted entropy with probability segmentation which takes into consideration the vascular influence on segmentation and current segmentation situation. Based on the vascular property that gray-level profile of the vascular cross section can be approximated by a Gaussian-shaped curve [2], Luo [13] proposed a two-dimensional amplitude-modified second-order differential matched filter for retinal vascular network detection. In our segmentation, a two-dimensional first-order partial differential matched filter is introduced to differentiate lesions from vascular network in abnormal images, which is proved to have better performance than second-order differential in our paper. Also it can automatically detect vascular network without any initial information and requires much less computational time because of its lower complexity compared with tracking-based and active contour model methods. In the process of proposed method, the homomorphic filter and two-dimensional matched filter are firstly applied to enhance the original image. Then a local adaptive segmentation using an weighted entropy with probability and two-dimensional partial differential matched filter is introduced to optimize the threshold value. Thus, each pixel in the image will be identified whether belonged to vascular network or not according to its local adaptive threshold value.

The remainder of this paper is organized as follows. Section II introduces the second-order entropy of an image. Section III then represents the main framework of proposed algorithm. Experimental evaluation results are illustrated in section IV. The last section concludes the works in this paper.

## II. SECOND-ORDER ENTROPY OF AN IMAGE

As the image pixel intensities are not independent of each other, we use the entropy of an image based on the gray-level co-occurrence matrix (GLCM) for the following segmentation. The GLCM can reflect the integrated information about direction, adjacent spacing and amplitude of variation. GLCM was defined by Haralick et al. in 1973 [15]. It shows how often a pixel value known as the reference pixel with the intensity value  $i$  occurs in a specific relationship to a pixel value known as the neighbour pixel with the intensity value  $j$ . So, each element  $(i, j)$  of the matrix is the number of occurrences of the pair of pixel with value  $i$  and a pixel with value  $j$  which are at a distance  $d$  relative to each other.

Suppose  $f(x, y)$  is an image gray-level function of size  $M \times N$ , for a displacement vector  $d = (d_x, d_y)$ , the gray-level co-occurrence matrix  $D$  can be defined as

$$D_{L \times L}(i, j) = \sum_{x=1}^M \sum_{y=1}^N \delta \quad (1)$$

$$\text{where } \begin{cases} \delta = 1 & \text{if } f(x, y) = i \text{ and } f(x + d_x, y + d_y) = j \\ \delta = 0 & \text{if otherwise} \end{cases}$$

$$i, j = 0, 1, \dots, L - 1.$$

and  $L$  is the gray levels, which is 256 in this paper and we define  $d = [0 \ 1]$  for horizontal direction and  $d = [-1 \ 0]$  for vertical direction. The probability of co-occurrence  $p(i, j)$  of gray levels  $i$  and  $j$  can therefore be written as

$$p(i, j) = \frac{D(i, j)}{\sum_i \sum_j D(i, j)} \quad (2)$$

$$\text{where } \sum_{i=0}^{L-1} \sum_{j=0}^{L-1} p(i, j) = 1 \text{ and } 0 \leq p(i, j) \leq 1$$

$$i, j = 0, 1, \dots, L - 1.$$

Hence we can define the second-order entropy of the image  $f(x, y)$  as

$$H_f = -\frac{1}{2} \sum_{i=0}^{L-1} \sum_{j=0}^{L-1} (p(i, j) / P) \ln (p(i, j) / P) \quad (3)$$

$$\text{where } P = \sum_{i=0}^{L-1} \sum_{j=0}^{L-1} p(i, j), \quad i, j = 0, 1, \dots, L - 1$$

## III. A LOCAL ADAPTIVE SEGMENTATION OF VASCULAR NETWORK FROM ABNORMAL RETINAL IMAGES

The overall framework of the proposed local adaptive segmentation (LAS) of vascular network from abnormal retinal images is illustrated in Fig. 1. The system takes as input the retinal gray-level image and returns the vascular network. From the input retinal image, the field of view (FOV) will be detected and then the image is pre-processed for following segmentation, including homomorphic filtering and two-dimensional matched filtering. Then an weighed entropy with probability segmentation is proposed to obtain preliminary vascular network, which contain lesions in abnormal retinal images. To address the problem, a local adaptive segmentation using two-dimensional partial differential matched filter is introduced to differentiate lesions from vascular network. An example of processing result is showed in Fig. 4.

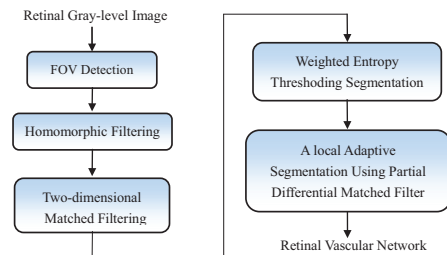


Fig. 1. Main steps of the proposed local adaptive segmentation (LAS) of vascular network from abnormal retinal images.

### A. FOV Detection

We can analyse the histogram of gray-level image to get the field of view (FOV). We firstly obtain all minimums on the histogram and make the minimum, when the area ratio of FOV is the nearest to a fixed ratio, as threshold value to

segment gray-level image. Fig. 4 (A4) illustrates the result of FOV detection and the fixed area ratio of FOV is set as 0.73.

### B. Image Pre-processing

1) *Homomorphic Filtering*: As the retina image has a great dynamic range of gray-level and the vascular brightness in retinal image are very dark, it is difficult to identify vascular details. It will be not enough just using the general linear gray-scale transforms to enhance the image. This paper uses homomorphic filtering which belongs to frequency domain processing. It can adjust the range of gray-level and eliminate uneven illumination in order to enhance image details in dark areas without losing details in bright areas. Fig. 4 (B1) shows the result of homomorphic filtering from the gray image in Fig. 4 (A2).

2) *Two-dimensional Matched Filtering*: To further enhance local contrast of the image, a two-dimensional matched filter is applied after homomorphic filtering. In signal processing, a matched filter is the optimal linear filter for maximizing the signal to noise ratio (SNR) with the additive white noise in the image. The idea of the matched filter [2] is introduced into retinal vascular detection based on the property that vascular gray-level profile of the cross section in a retinal image can be approximated by a Gaussian-shaped curve and some other properties like

- Vessels have small curvatures so that can be approximated as anti-parallel pairs and piecewise linear segments.
- Vessels appear darker than background because of lower reflectance.
- Width of a vessel decreases gradually outward from the optic disk, which is found to lie within the range of 2-10 pixels.

Fig. 2 shows several gray-level profiles of cross section in a retinal image.

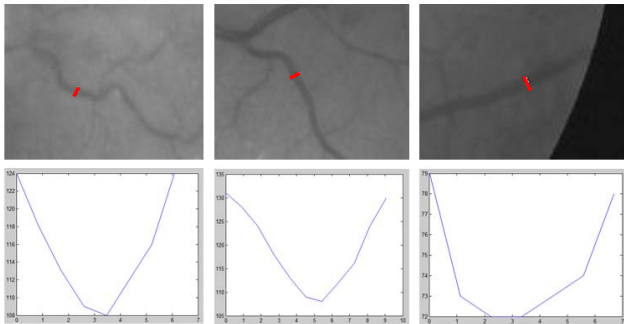


Fig. 2. Several vascular gray-level profiles of cross section in retinal image.

Therefore, the two-dimensional matched filter is designed to enhance the local contrast of vascular network.

Define a neighborhood  $Q = \{|x| \leq 3\sigma, |y| \leq L/2\}$ ,  $\sigma$  is the scale of filter and  $L$  is the length of segment where the vascular direction is assumed to be fixed, which is along  $y$ -axis

in this paper. The corresponding two-dimensional matched filter kernel  $h$  is defined as

$$h(x, y) = -\frac{1}{\sqrt{2\pi}\sigma} \exp\left(-\frac{x^2}{2\sigma^2}\right) \quad (4)$$

If  $A$  is the number of points in  $Q$ , the mean value of  $h$  is calculated as

$$m = \sum h(x, y) / A \quad (5)$$

Thus the matched filter kernel used in this paper is

$$k(x, y) = h(x, y) - m \quad (6)$$

Then the kernel will be rotated for different orientations since the vascular direction is not sure. Fig. 4 (B2) shows the response image to two-dimensional matched filter of Gaussian shape with the parameters  $(L, s) = (9, 2)$  from the image showed in Fig. 4 (B1).

### C. Weighted Entropy Segmentation

To obtain the optimal or suboptimal threshold value for vascular segmentation, entropy is employed in the paper. As mentioned in section II, the second-order entropy based on gray-level co-occurrence matrix (GLCM), which is defined as equation (1), is applied for segmentation. Suppose that  $s$ ,  $0 \leq s \leq L-1$ , is a threshold value and it will divide the GLCM into four areas. They respectively correspond to the object, background, edges and noises. As to a pixel belonging to object or background, its gray level is similar to that of its neighbours. On the contrary, gray level of a pixel belonging to edges or noises is greatly different from that of its neighbours. Suppose that area  $A$  and  $B$  represent object or background and area  $C$  and  $D$  represent edges or noises. The second-order entropy of area  $A$  is

$$H_A(s) = -\frac{1}{2} \sum_{i=0}^s \sum_{j=0}^s (p(i, j)/p_A) \ln(p(i, j)/p_A) \quad (7)$$

And the second-order entropy of area  $B$  is

$$H_B(s) = -\frac{1}{2} \sum_{i=s+1}^{L-1} \sum_{j=s+1}^{L-1} (p(i, j)/p_B) \ln(p(i, j)/p_B) \quad (8)$$

Where

$$\begin{aligned} p_A &= \sum_{i=0}^s \sum_{j=0}^s p(i, j) \\ p(i, j)/p_A &= \frac{D(i, j)}{\sum_{i=0}^s \sum_{j=0}^s D(i, j)} \\ \text{for } &0 \leq i \leq s, 0 \leq j \leq s \end{aligned} \quad (9)$$

and

$$\begin{aligned} p_B &= \sum_{i=s+1}^{L-1} \sum_{j=s+1}^{L-1} p(i, j) \\ p(i, j)/p_B &= \frac{D(i, j)}{\sum_{i=s+1}^{L-1} \sum_{j=s+1}^{L-1} D(i, j)} \\ \text{for } &s+1 \leq i \leq L-1, s+1 \leq j \leq L-1 \end{aligned} \quad (10)$$

Because the number of pixels of edges and noises is of a very small proportion, the second-order entropy of area C and D can be left out.  $H_f$  is total second-order entropy of the whole

image and we want to make the sum of  $H_A(s)$  and  $H_B(s)$  is the nearest to  $H_f$ , that means

$$H(s) = H_f - (H_A(s) + H_B(s)) \quad (11)$$

can reach its minimum value. Therefore the gray level  $s^*$  reaching the minimum of  $H(s)$  is the optimal global threshold value for segmentation. Denote the segmentation result by  $I_s$ .

The minimum entropy thresholding is based on assumption that the object and background have uniform probability distribution. However, it only uses the image intensity distribution, without taking into account the spatial relationships between adjacent pixels, so that the segmentation result is not satisfactory to some extent. Therefore, we introduce a weighted entropy

$$H_A(s) = -\frac{1}{2} \sum_{i=0}^s \sum_{j=0}^s w(i, j) (p(i, j) / p_A) \ln(p(i, j) / p_A) \quad (12)$$

$$H_B(s) = -\frac{1}{2} \sum_{i=s+1}^{L-1} \sum_{j=s+1}^{L-1} w(i, j) (p(i, j) / p_B) \ln(p(i, j) / p_B) \quad (13)$$

Here,  $w(i, j) \geq 0$  is the weight coefficient and it is defined based on the probability corresponding with equation (1), which can be calculated by

$$T_{L \times L}(i, j) = \sum_{x=1}^M \sum_{y=1}^N \delta' \quad (14)$$

$$\text{where } \begin{cases} \delta' = 1 & \text{if } f(x, y) = i, f(x + d_x, y + d_y) = j \\ & \text{and } I_s(x, y) = 1 \\ \delta' = 0 & \text{if otherwise} \end{cases}$$

$$w(i, j) = \left( \frac{T(i, j)}{M(i, j)} \right)^k, \quad 0 \leq k \leq 1 \quad (15)$$

Then normalize the  $w(i, j)$  to  $[0, 1]$ . When  $k = 0$ , equation (12) and equation (13) are same with equation (7) and equation (8).  $w(i, j)$  will be larger when  $P(i, j)$  is larger and hence it can increase the vascular influence on the segmentation. Also it takes into consideration the current segmentation situation. As to the optimal value of  $k$ , it can make the contrast of object and background reach the maximum. The contrast of object and background can be defined as

$$C_k = |G_o - G_b| / (G_o + G_b) \quad (16)$$

where  $G_o$  is the average gray value of object and  $G_b$  is the average gray value of background. Fig. 4 (C1) shows the result of advanced thresholding segmentation from Fig. 4 (B2).

#### D. Local Adaptive Segmentation

From the Fig. 4 (C1) we can see the lesions are segmented into vascular network, which is due to that the lesions also have high response to the two-dimensional matched filter when image pre-processing. To overcome the issue, a local adaptive segmentation (LAS) using two-dimensional partial differential matched filter (TPDMF) is introduced into segmentation in following. The two-dimensional matched filter kernel is defined as equation (6), and its partial differential for  $x$  is defined as

$$k_x(x, y) = \frac{x}{\sqrt{2\pi}\sigma^3} \exp\left(-\frac{x^2}{2\sigma^2}\right) \quad (17)$$

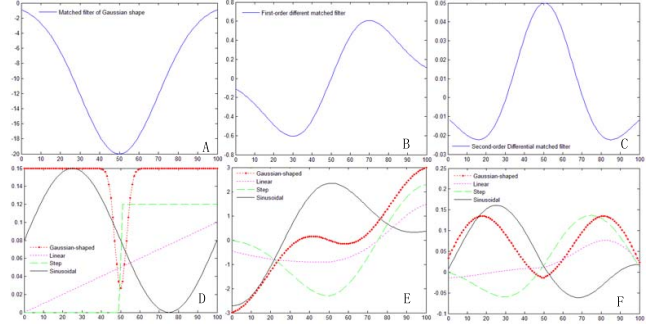


Fig. 3. The responses to differential matched filters for different kinds of signals. (A) Matched filter of Gaussian shape. (B) First-order differential of (A). (C) Second-order differential of (A). (D) Different kinds of signals. (E) The signal responses to (B). (F) The signal responses to (C).

Fig. 3 shows the responses to first-order and second-order differential matched filters for different kinds of signals, which are shown in (D), including Gaussian-shaped signal, linear signal, step signal and sinusoidal signal. The Gaussian-shaped signal is used to simulate the vascular profile, while the linear, step and sinusoidal signals are used to simulate the lesions which may appear in various change because of their irregular shapes. (B) and (C) are the first-order and second-order differential of (A). (E) and (F) are the signal responses to (B) and (C) respectively. In (E), the response of Gaussian-shaped signal is equal to zero at the center position ( $x = 50$ ), which is simulated as the center of vascular profile, and close to zero around the center. Only the position around center is considered here because the neighbourhood  $Q$  of matched filter defined as equation (6) is not wide. In contrast, the absolute value of responses for other signals around the center are high. Thus, it is easy to differentiate them by first-order differential matched filter. In (F), the responses of linear, step and sinusoidal signals are positive on one side of center and negative on another side. And their absolute values are similar to the absolute value of Gaussian-shaped signal response. Thus, it is difficult to differentiate them by second-order differential matched filter. Therefore, a two-dimensional first-order partial differential matched filter is applied in our segmentation to differentiate the lesions from vascular network.

Denote the response image to two-dimensional partial differential matched filter from homomorphic filtering image by  $f_p(x, y)$ . Therefore, the local adaptive threshold value for segmentation can be defined as

$$t_l^*(i, j) = s^* + \lambda \cdot |f_p(i, j)|, \quad i, j = 0, 1, \dots, L-1 \quad (18)$$

As to a pixel  $(i, j)$  belonging to vascular network in the image, its response absolute value  $|f_p(i, j)|$  is very small and thus its corresponding local adaptive threshold value  $t_l^*(i, j)$  will be low. On the contrary, the local adaptive threshold value of a pixels belonging to lesions is high and consequently it is harder to be segmented into vascular network.

The response image of Fig. 4 (B1) is showed in Fig. 4 (B3). Fig. 4 (C2) shows the result after using the partial differential matched filter. Moreover, the difference between Fig. 4 (C1) and (C2) can be regarded as lesions, which is showed as Fig. 4 (C3). In practice we discover that segmentation for the image after processing partial different matched filter can



obtain more thin vessels. Therefore, we will combine it with the segmentation in Fig. 4 (C2) to obtain the resultant vascular network showed in Fig. 4 (C4).

#### IV. EXPERIMENTAL RESULTS

##### A. Material

Our method is evaluated on the publicly available database, STARE [17]. The database consists of twenty images, ten of which are normal and the other then abnormal. The images were captured in digital form by a TopCon TRV-50 fundus camera at  $35^\circ$  field of view. Each image to be analysed is  $700 \times 600$  pixels in size and 24 bits for per pixel. And manual vascular network segmentation by two experts are also available for measurement and comparison. In our experiments, manual segmentation from the first human expert will regarded as the gold-standard image (GSI).

##### B. Metrics

In order to quantify the algorithmic performance of the our method on a retinal image, the resulting segmentation is compared to its corresponding gold-standard image (GSI) which is examined by the first human expert. Thus, automated vascular segmentation performance can be assessed and compared with other methods. In this paper, we select TPR (true positive rate), FPR (false positive rate), ACC (accuracy) and QF (quality factor) as our performance measures, which are widely used in the literature. According to table I, they are defined as

$$TPR = \frac{TP}{TP + FN} \quad (19)$$

$$ACC = \frac{TP + TN}{TP + FN + FP + TN} \quad (20)$$

$$QF = \frac{TP}{TP + FN} - \frac{FP}{FP + TN} \quad (21)$$

TABLE I. CONTINGENCY VASCULAR CLASSIFICATION.

	Vessels present in GSI	Vessels absent in GSI
Vessels detected	True Positive (TP)	False Positive (FP)
Vessels not detected	False Negative (FN)	True Negative (TN)

##### C. Vascular Network Detection Result

We test our method on each original retinal image in STARE database by the steps described in Section III with matlab R2013b. An example of an original and abnormal RGB retinal image "im0001" taken from STARE database is showed in Fig. 4. (A1) is the original RGB image and (A2) is the gray-level image of (A1), which is taken as the input of our method. (A3) is the histogram of (A2) and the detected FOV is showed in (A4). (B1) is the homomorphic filtering image and its matched filter response image, TPDMF response image are showed in (B2) and (B3) respectively. (B4) is the manual vascular segmentation which is regarded as GSI. (C1) is the segmentation of (B2) and its result using TPDMF is showed in (C2) and the lesions is in (C3). The resultant vascular network detected are showed in (C4).

As we can not obtain detailed results from some of methods introduced in Introduction, these method will not be taken into comparison. Fig. 5 showed the vascular network segmentation

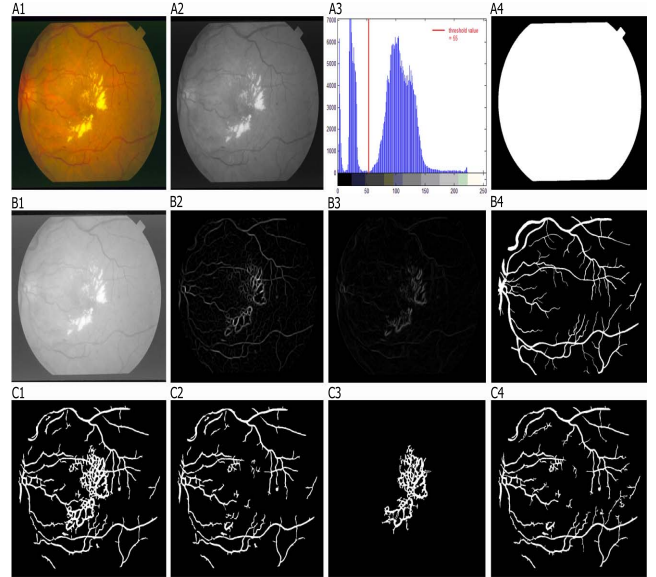


Fig. 4. Overview of main steps of proposed method on an original and abnormal RGB retinal image "im0001" taken from STARE database.

results compared with other methods on abnormal retinal images. The first column is the original RGB retinal images taken from STARE which are abnormal and the second column is the gold-standard images. The third one is result of Sumathy's method [12] and next one is result of Hoover's method [17]. Our detection are showed in the last column. By comparison, we can see that our method can differentiate lesions from vascular network more accurately and obtain more vascular details as well.

##### D. Weighted Entropy Thresholding Segmentation Analysis

Fig. 6 aims to demonstrate the performance of the segmentation by our proposed weighted entropy thresholding segmentation. We firstly get the two-dimensional matched filter output image denoted by  $f_{TMF}$  with the parameters for  $(L, \sigma) = (9, 2)$  as originally proposed in [2]. And then we will obtain several binary images by thresholding  $f_{TMF}$  via different threshold value from 0 to 255 in a step of 4. The TPR and ACC will be calculated for each image and we can obtain QF to judge the quality of image. Then we will undertake the proposed weighted entropy segmentation (without using two-dimensional partial differential matched filter) on  $f_{TMF}$  and get a threshold value. The resultant curves are shown in Fig. 6. From the result we can see that our weighted entropy threshold value approximates the optimal value when QF reaches its maximum. Meanwhile the ACC is close to its maximum.

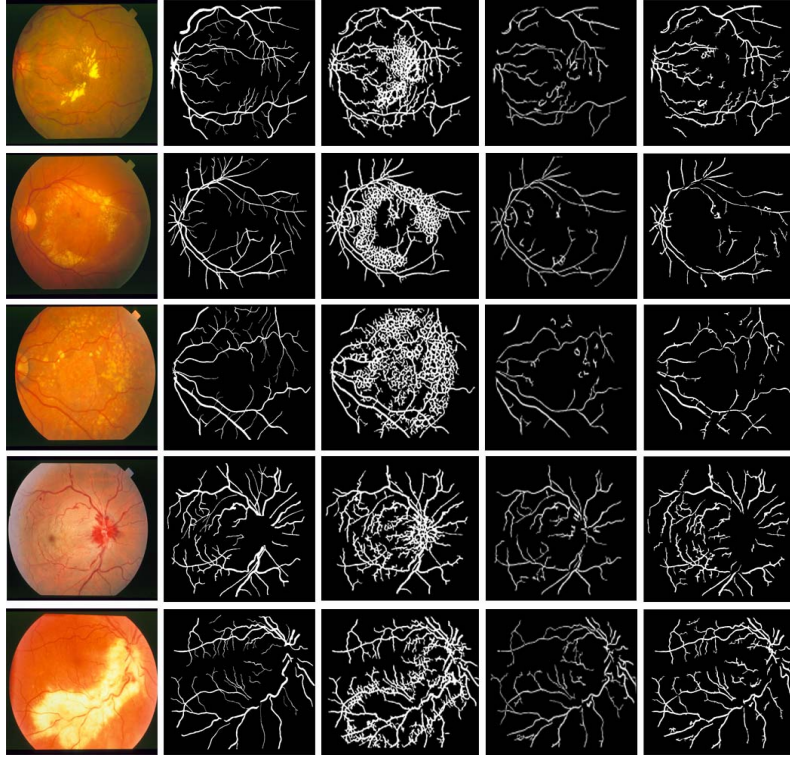


Fig. 5. Comparison of vascular detection. The first column is the original RGB retinal images and second one is the gold-standard images. The results of Sumathy's method [12], Hoover's method [17] and our method are showed in the last three columns.

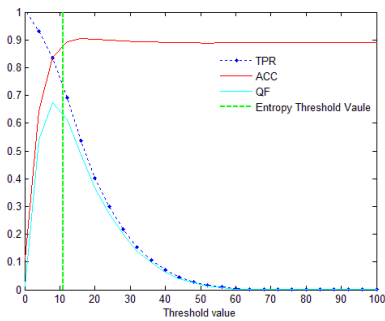


Fig. 6. The curves of TPR, FPR, ACC, QF and obtained threshold value by weighted entropy thresholding segmentation of "im0001".

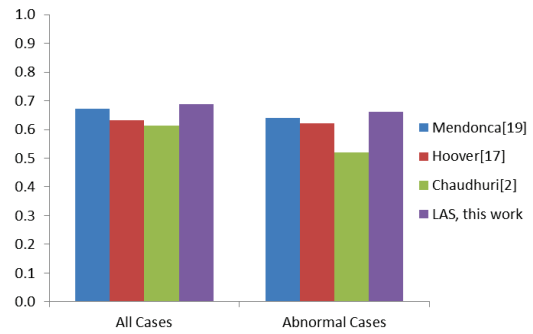


Fig. 8. Comparison results in term of QF.

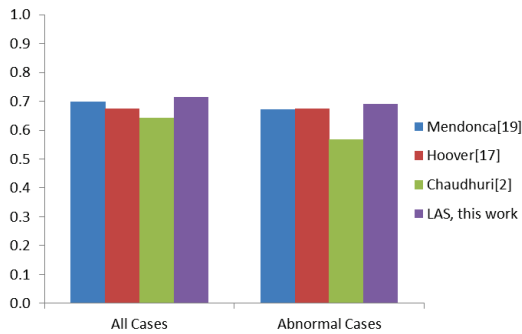


Fig. 7. Comparison results in term of TPR.

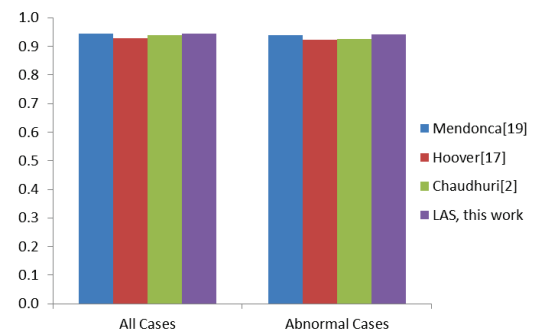


Fig. 9. Comparison results in term of ACC.

### E. Vascular Detection Result Comparison

Fig. 7, Fig. 8 and Fig. 9 present the comparison results between our proposed local adaptive segmentation (LAS) and other state-of-the-art methods on all cases (10 normal images and 10 abnormal images) and abnormal cases (10 abnormal images) in STARE database respectively in terms of TPR, QF and ACC. The result of Mendonca [19] comes from its paper and those of Chaudhuri [2] and Hoover [17] are obtained by calculating their resultant images. Some other methods which can obtain their results only on all cases will not be listed in the figure. From the figure, we can tell that our method get better performance in terms of both TPR, QF and ACC compared with other methods. Specially, it can improve the performance on abnormal images as well. Since the abnormal images have lesions that can not be removed completely in the segmentation, the performance on abnormal cases is worse than that on all cases. However the increasement on abnormal cases is larger. In term of TPR on all cases, the increasement is 1.02% compared with the best one of other three methods and average increasement is 4.77%, which are smaller than those on only abnormal cases, 2.35% and 8.75% respectively. And the same conclusion come to QF and ACC. Among the three metrics, QF obtains the largest increasement, which means our method can improve the quality of vascular segmentation efficiently, and ACC obtains the smallest increasement because the results of other three methods in term of ACC are good enough.

### V. CONCLUSION

This paper proposed a local adaptive segmentation of vascular network from abnormal retinal images. In the first stage, the image is pre-processed by a homomorphic filter and a two-dimensional matched filter, which is based on the vascular property that vascular gray-level profile of the cross section can be approximated by a Gaussian-shaped curve. Then the local adaptive segmentation using weighted entropy and two-dimensional partial differential matched filter is introduced to determine the optimal local adaptive threshold value to segment for each pixel in the image. The proposed algorithm is compared to several vascular network segmentation algorithms on STARE and it comes to the conclusion that our method can reach better performance.

### REFERENCES

- [1] Chanwimaluang, Thitiporn, and Guoliang Fan. "An efficient algorithm for extraction of anatomical structures in retinal images." *Image Processing, 2003. ICIP 2003. Proceedings. 2003 International Conference on*. Vol. 1. IEEE, 2003.
- [2] Chaudhuri, Subhasis, et al. "Detection of blood vessels in retinal images using two-dimensional matched filters." *IEEE transactions on medical imaging* 8.3 (1989): 263-269.
- [3] Lin, Kai-Shun, et al. "Retinal vascular tree reconstruction with anatomical realism." *Biomedical Engineering, IEEE Transactions on* 59.12 (2012): 3337-3347.
- [4] Freeman, William T., and Edward H. Adelson. "The design and use of steerable filters." *IEEE Transactions on Pattern analysis and machine intelligence* 13.9 (1991): 891-906.
- [5] Zana, Frdric, and J-C. Klein. "Robust segmentation of vessels from retinal angiography." *Digital Signal Processing Proceedings, 1997. DSP 97., 1997 13th International Conference on*. Vol. 2. IEEE, 1997.
- [6] Lau, Qiangfeng Peter, et al. "Simultaneously identifying all true vessels from segmented retinal images." *IEEE Transactions on Biomedical Engineering* 50.7 (2013): 1851 - 1858.
- [7] Wu, Chang-Hua, Gady Agam, and Peter Stanchev. "A general framework for vessel segmentation in retinal images." *Computational Intelligence in Robotics and Automation, 2007. CIRA 2007. International Symposium on*. IEEE, 2007.
- [8] Staal, Joes, et al. "Ridge-based vessel segmentation in color images of the retina." *Medical Imaging, IEEE Transactions on* 23.4 (2004): 501-509.
- [9] Tramontan, Lara, et al. "A web-based system for the quantitative and reproducible assessment of clinical indexes from the retinal vasculature." *Biomedical Engineering, IEEE Transactions on* 58.3 (2011): 818-821.
- [10] Shang, Yanfeng, et al. "Vascular active contour for vessel tree segmentation." *Biomedical Engineering, IEEE Transactions on* 58.4 (2011): 1023-1032.
- [11] Sun, Kaiqiong, Zhen Chen, and Shaofeng Jiang. "Local morphology fitting active contour for automatic vascular segmentation." *Biomedical Engineering, IEEE Transactions on* 59.2 (2012): 464-473.
- [12] Sumathy, B., and S. Poornachandra. "Retinal blood vessel segmentation using morphological structuring element and entropy thresholding." *Computing Communication & Networking Technologies (ICCCNT), 2012 Third International Conference on*. IEEE, 2012.
- [13] Gang, Luo, Opas Chutatape, and Shankar M. Krishnan. "Detection and measurement of retinal vessels in fundus images using amplitude modified second-order Gaussian filter." *Biomedical Engineering, IEEE Transactions on* 49.2 (2002): 168-172.
- [14] Hsiao, Ying-Tung, et al. "Robust multiple objects tracking using image segmentation and trajectory estimation scheme in video frames." *Image and Vision Computing* 24.10 (2006): 1123-1136.
- [15] Haralick, Robert M., Karthikeyan Shanmugam, and Its' Hak Dinstein. "Textural features for image classification." *Systems, Man and Cybernetics, IEEE Transactions on* 6 (1973): 610-621.
- [16] Bankhead, Peter, et al. "Fast retinal vessel detection and measurement using wavelets and edge location refinement." *PloS one* 7.3 (2012): e32435.
- [17] Hoover, Adam, Valentina Kouznetsova, and Michael Goldbaum. "Locating blood vessels in retinal images by piecewise threshold probing of a matched filter response." *Medical Imaging, IEEE Transactions on* 19.3 (2000): 203-210.
- [18] Martinez-Perez, M. Elena, et al. "Segmentation of blood vessels from red-free and fluorescein retinal images." *Medical Image Analysis* 11.1 (2007): 47-61.
- [19] Mendonca, Ana Maria, and Aurelio Campilho. "Segmentation of retinal blood vessels by combining the detection of centerlines and morphological reconstruction." *Medical Imaging, IEEE Transactions on* 25.9 (2006): 1200-1213.
- [20] Soares, Joao VB, et al. "Retinal vessel segmentation using the 2-D Gabor wavelet and supervised classification." *Medical Imaging, IEEE Transactions on* 25.9 (2006): 1214-1222.
- [21] Cinsdikici, Muhammed Gkhan, and Dogan Aydin. "Detection of blood vessels in ophthalmoscope images using MF/ant (matched filter/ant colony) algorithm." *Computer methods and programs in biomedicine* 96.2 (2009): 85-95.
- [22] Perfetti, Renzo, et al. "Cellular neural networks with virtual template expansion for retinal vessel segmentation." *Circuits and Systems II: Express Briefs, IEEE Transactions on* 54.2 (2007): 141-145.